

Evolution of Bipartiteness in Networks

Sarika Jalan^{1,2} * and Sanjiv K. Dwivedi¹

1. *Complex Systems Lab, Physics Discipline, Indian Institute of Technology Indore, Khandwa Road, Indore 452017, India* and
 2. *Center for Biosciences and Biomedical Engineering,
 Indian Institute of Technology Indore, Khandwa Road, Indore 452017, India*

Bipartite interaction patterns are commonly observed in real world systems which we hypothesize here as an efficient structural interaction pattern naturally arising in the course of evolution. We demonstrate that a random structure evolves to the bipartite structure by imposing stability criterion through minimization of the largest eigenvalue in the genetic algorithm. The bipartite structure emerges as the final evolved structure while taking invariant nature of interaction behavior of interacting units. The evolved interaction patterns are robust against changes in the initial network architecture as well as fluctuations in the interaction weights.

PACS numbers: 89.75.Hc,02.10.Yn

I. INTRODUCTION

Finding mechanisms governing the evolution of patterns in real world systems remains challenging in the evolutionary science [1]. Structural pattern of a network not only influences the functional response [2], but also is motivated from a specific function of the corresponding system [3]. Since external perturbations, occurring due to various reasons, may have impact on specific functions of a system [4, 5], various different structural patterns have been emphasized for maintaining these functions. For instance, the scale-free structure makes a network robust against random attack [6]. Small-world structure, while demonstrating high clustering, facilitates a fast spread of information [7]. Motif structures are known to provide functional robustness to a system [8]. Exploring evolutionary origins of existing structures is important to develop an understanding pertaining to the hidden roles of these structures. For example, nestedness in ecological networks structure has been shown as an evolved property in co-operative interactions [9] and also in maximizing the structural stability of mutualistic systems [10, 11].

In the present work, we focus on understanding the evolutionary origin of bipartiteness and multipartiteness in real world networks. A network is called bipartite if its nodes can be divided into two groups in such a manner that nodes in one group are connected to the nodes in the second group with no connection existing within the same group. In a multipartite network, there are several communities which are either not connected or very sparsely connected among themselves. There are many natural systems which yield bipartite (or multipartite) network structures. Few examples of the real world networks, which are build up to the current state as a result of evolution and possess the bipartite (or multipartite) structure, are gene regulatory interaction networks con-

sisting of two groups of regulating and regulated genes [12], ecological food webs having different trophic levels [13, 14], EI Verde rainforest [15], etc.

Additionally, several systems are known to be characterized by their constituents defined by different behaviors. For example, according to Dale's principle, in a neural system all outgoing synapses of a neuron are either inhibitory (I) or excitatory (E) [16], thereby leading to various structural properties due to I-E, I-I and E-E couplings [17, 18]. Whereas, in ecosystem, several species show bias for the mixed behavior. For example, Apex predators have zero or less number of predators for their own community [19]. These different behaviors of nodes or interactions are crucial for a desired functioning or the robust functional performance of the underlying system. For instance, despite high degree of complexity, the abundance of predator-prey interactions confer stability to the systems [5, 20].

In the context of ecological systems, the celebrated work by Robert May demonstrates that the largest real part of eigenvalues (R_{\max}) of the corresponding Jacobian matrices contain information about the stability of the underlying systems [21]. The emergence of complex structural properties during the growth process has been studied using R_{\max} as a stability selection criteria [22]. Further, the Genetic algorithm (GA) is a widely used technique in optimization problems as well as in providing evolutionary models for systems in many disciplines [23, 24]. It has been shown that a stability maximization-based genetic algorithm leads to an emergence of the hierarchical modularity in a network [4]. Recently, evolution of clustering is demonstrated by maximizing the stability of the underlying network using GA [25]. This paper provides an explanation to the emergence of bipartite (multipartite) structure using GA-based minimization of R_{\max} .

II. THEORETICAL FRAMEWORK

We start with the P independently drawn adjacency matrices, $[a_{ij}]$ (each having dimension N) corresponding

*Corresponding author:sarikajalan9@gmail.com

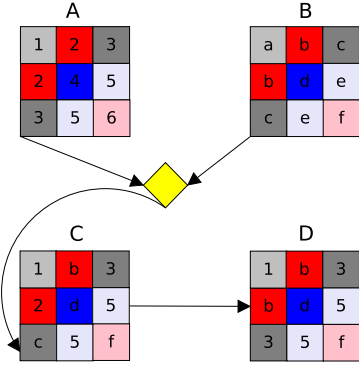


FIG. 1: (Color online) Mechanism to generate a child matrix from a pair of randomly selected fitter networks. The blocks of the parent and child matrices at a particular position are represented with the same color. The dimension of each of these square blocks is 10. Note that the GA works fine for all the block sizes significantly less than N . For larger block size, GA becomes meaningless as the child matrices lose variability and turn out to be very similar to their parent matrices.

to Erdős-Rényi (ER) random networks representing the initial population. Elements in the corresponding adjacency matrices $[a_{ij}]$ take value 1 and 0 depending upon whether there exists a connection between i th and j th nodes which is decided with a probability q . Next we generate matrices in which each node is either excitatory (type-I) or inhibitory (type-II) throughout the evolution. This is motivated from the Jacobian (synaptic) matrices considered in the model of [26], which incorporates Dale's principle. Such type of matrices have following properties: (i) The columns are either Gaussian distributed numbers with negative mean or positive mean with certain variance. (ii) Summation of the numbers in each row is equal to zero, which takes into account the balanced condition. Such matrices lead to the underlying networks that are globally connected. Therefore, with probability p_{in} , type-II nodes (i.e. nodes with only I connections) are randomly selected out of the total N nodes (Eq. 1). Rest of the nodes form a set of the type-I nodes (i.e. nodes with only E connections) of the behavior matrices. This arrangement leads to the following matrix, termed as behavior matrix, which has a balance of the inhibition and excitation [26, 27] in the whole network,

$$b_{ij} = \begin{cases} 1 - 1/p_{in} \forall j, & \text{if } i \in \text{type-II} \\ 1 & \forall j, \text{ if } i \in \text{type-I} \end{cases} \quad (1)$$

More specifically in Eq. 1, rows of matrices $[b_{ij}]$ have either '+1' or ' $1 - 1/p_{in}$ ' entries. The entries of the b_{ij} matrices are fixed in the course of evolution, demonstrating the invariant nature of nodes and consequently the links [28]. We define another matrix $[c_{ij}]$ (Eq. 2) for assessing the fitness of a network, which is constructed using the adjacency matrices of the network and the behavior

matrix (Eq. 1) in the following manner:

$$c_{ij} = \begin{cases} b_{ij} & \text{if } a_{ij} \neq 0 \\ 0 & \text{otherwise} \end{cases} \quad (2)$$

A network corresponding to lower R_{\max} value of an associated $[c_{ij}]$ matrix is referred here as a fitter network. For the next generation, the P fitter networks of size $N \times N$ each are created as follows. First of all we select $P/2$ number of distinct networks from these networks which have R_{\max} values lesser than those of the rest of the networks in the present population. These selected networks are fitter networks and act as the parent networks for creating rest $P/2$ child networks for the next generation (Fig. 1). For example, in order to generate one child (say C), a pair of networks (say A and B) from $P/2$ population are selected randomly. Then each block of the adjacency matrix of the child at a specified dimension and location (in terms of rows and columns), is filled with the block having the same position in the parent matrices, with an equal probability (Fig. 1). The child matrices generated are asymmetric in nature. We thus take the upper triangular part of the child matrices and construct their adjacency matrix such that they are symmetric. In order to avoid trivial changes in the R_{\max} values due to the change in the total number of connections in the network and to get a signature of the change in the network pattern on the R_{\max} values, we preserve the average degree ($\langle k \rangle$) of the child matrices by randomly removing or inserting connections with a small probability. This probability is decided by the fluctuation of the average degree in the crossed child network from the degree of the initial networks population used in the GA. Thus, the total number of edges remain almost same for the child networks.

In order to emphasize that here changes in the value of R_{\max} are not due to the change in the average degree [29] but arising due to the changes in the interaction patterns, we present the results for the preserved average degree of the child network. Since real networks are known to be sparse in nature, the results are presented for $\langle k \rangle = 6$. A lesser value of $\langle k \rangle$ leads to disconnected components, in turn affecting R_{\max} . With an increase in $\langle k \rangle$, R_{\max} increases in general. The larger $\langle k \rangle$ leads to a less variation among the structural conformations of initial network population, which results in a lesser variation in the child population as well. The small amount of variation present in the set of initial networks population vanishes after certain generations without producing sufficient structural changes with respect to the initial population. The evolution stops when there is no structural variation in the network population. Also bipartite structure does not exist for a network having $\langle k \rangle > N/2$. Thus, the GA approach which preserves the average degree, does not lead to evolution of bipartite structure for very dense networks. Further, with larger N , the values of R_{\max} may vary but the overall behavior that R_{\max} minimization leads to evolution of the bipartiteness is expected to remain same, provided the initial

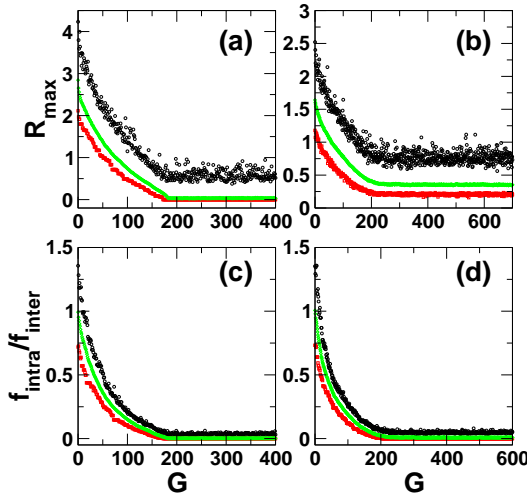


FIG. 2: (Color online) (a) and (c) plot evolution of R_{\max} and $f_{\text{intra}}/f_{\text{inter}}$ respectively for $p_{\text{in}} = 0.50$ and connection weight from Eq. (1). Minimum, average and maximum values for the network population are indicated by \square (red), \diamond (green) and \circ (black) respectively. (b) and (d) depict evolution of R_{\max} and $f_{\text{intra}}/f_{\text{inter}}$, respectively for connection weight with fluctuations as imposed by Eq. (2). Initial ER networks have $\langle k \rangle = 6$ with $N = 100$. For all the cases network population is 500.

networks consists of different types of nodes. The problem encountered on considering larger network size [4], would be requirement of memory allocation for a population of P networks in GA amounting to PN^2 size of the 1-d array, which is computationally not favorable for large N .

Further, the total number of connections within the same population (within type-I or within type-II) is denoted by f_{intra} and the total number of connections among the different populations (between type-I and type-II) is denoted by f_{inter} . The ratio of f_{intra} and f_{inter} provides a measure for the bipartivity [30, 31]. The zero value of $f_{\text{intra}}/f_{\text{inter}}$ indicates a bipartite structure. However the converse is not true, a bipartite structure might also arise when in a network, there are two groups of nodes such that one group (having both type-I and type-II category nodes) forms all the connections with the other group (again having both type-I and type-II category nodes) and no connection within the group. Connections between type-I and type-II nodes of individual groups would contribute to f_{intra} leading to non-zero $f_{\text{intra}}/f_{\text{inter}}$ value. Note that, a bipartite structure may exist in a system having only single behavior. For example, a system in which plants and pollinators form two different communities exhibiting the bipartite structure with only type-I couplings [9–11, 20]. This situation does not arise in our analysis as we consider different classes of nodes and bipartiteness is confirmed only when the value of $f_{\text{intra}}/f_{\text{inter}}$ is zero.

III. EMERGENCE OF BIPARTITE STRUCTURE

Starting with sparse ER random networks as an initial population, as evolution progresses through GA (Fig. 2), the minimization of R_{\max} occurs. In the initial population, the mean of $f_{\text{intra}}/f_{\text{inter}}$ is close to *one*, however maxima and minima are different as expected from the various realizations of the ER networks. As evolution progresses, the mean and minimum values of $f_{\text{intra}}/f_{\text{inter}}$ converge towards zero, however maxima still exhibits a small separation from the zero (Fig. 2). This indicates that most of the networks in the evolved population attain the bipartite structure in which no or a very few connections exist within type-I or within type-II category nodes. Since, the GA minimizes R_{\max} values of the population, the convergence of the maxima towards zero is stopped when the minima closely coincides with the mean value. What follows that the initial population consisting of random architecture (Fig. 3(a)) converges to the bipartite structure (Fig. 3(b)) through the stability maximization.

The emergence of the bipartite structure directly follows from the spectral properties of antisymmetric matrices entailing all imaginary eigenvalues. The $[c_{ij}]$ matrix, for a ideal bipartite structure without any connection within type-I or within type-II category nodes, corresponds to a antisymmetric matrix, i.e. $[c_{ij}] = -[c_{ji}]$. The R_{\max} of $[c_{ij}]$ for the initially considered ER networks, generated using connection probability q , takes positive values given by \sqrt{Nq} for $p_{\text{in}} = 0.50$ [32]. Additionally, the correlation in the elements of c matrix, given as $\tau = \sum_{i,j=1}^N c_{ij}c_{ji} / \sum_{i,j=1}^N c_{ij}c_{ij}$ for the matrices defined by Eq. 1, takes value

$$\tau = (f_{\text{intra}} - f_{\text{inter}}) / (f_{\text{intra}} + f_{\text{inter}}) \quad (3)$$

for $p_{\text{in}} = 0.5$. This value decreases with $f_{\text{intra}}/f_{\text{inter}}$, further leading to a decrease in R_{\max} because the spectral distribution of $[c_{ij}]$ matrices are of elliptical shape with its axis lying on the real line decreasing around a fixed center [33]. Since we minimize R_{\max} , the GA successfully and smoothly evolves a structure in which $f_{\text{intra}}/f_{\text{inter}}$

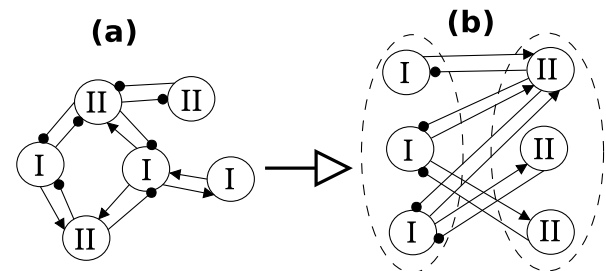


FIG. 3: (Color online) Schematic diagram for (a) initial population of ER networks and (b) finally evolved bipartite structure denoted with dashed circles. Dots and arrows represent I and E links, respectively.

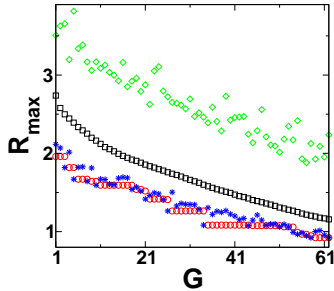


FIG. 4: (Color online) R_{\max} during the evolution of matrices $[c_{ij}]$ for children and parents population. Square (black) and circle (red) represent maxima and minima of R_{\max} values of the $[c_{ij}]$ matrices for the parents population respectively and diamond (green) and star (blue) are maxima and minima of R_{\max} values of $[c_{ij}]$ matrices for the children population respectively.

has very small or zero value.

The successful performance of the GA can be explained by considering two different classes of network population. Let the children and their parent populations form two different classes of networks in each generation and the R_{\max} of $[c_{ij}]$ associated with both the classes, decrease during the evolution. The maxima and minima of R_{\max} for the parent $[c_{ij}]$ decrease as per the GA minimization (Fig. 4). The maxima and minima of R_{\max} for children $[c_{ij}]$ also decrease with the evolution. It happens so that the maxima of R_{\max} values for children population is greater than the maxima of those for the parents population. The hamming distance between the adjacency matrices of networks provide a method to measure this dissimilarity [34]. What follows that, whenever parents exhibit dissimilarity, i.e. Hamming distance is large, their crossed child is also likely to have a high deviation in its structural properties which in turn leads to a large deviation of R_{\max} of the child from its parent.

Furthermore, the minima value for children and parents populations may lead to the following two cases. In the first case, the minima value for children is higher than the minima value for the parent population. Hence, the minima value for parent population in the subsequent generations does not decrease until the minima values for the children become lower than the minima value of their parents population. Whereas in the second case, the minima values for parents are higher than those of child, hence parents, which produce child for the next generation, are selected from the child in the current generation leading to a decrease in the minima of the parents for the next generation. This leads to the value of R_{\max} decreasing in each generation which indicates that as evolution progresses, the evolved feature (i.e. a lesser value of $f_{\text{intra}}/f_{\text{inter}}$) is transferred to the child. It occurs due to the procedure of block selection for child matrices as represented in the schematic diagram (Fig. 1). The GA-based optimization method converts the entries of the ad-

jacency matrices corresponding to the connections within type-I nodes and the connections within type-II nodes to E-I couplings, thus leading to a decrease in $f_{\text{intra}}/f_{\text{inter}}$ value. The decreased values of $f_{\text{intra}}/f_{\text{inter}}$ of parent matrices give rise to a chance to produce a child with a further decreased value. And whenever parents produce such type of child network, they possess lower R_{\max} values which are selected for the next generation. In other words, fitter children are produced by the fitter parents.

IV. ROBUSTNESS AGAINST RANDOM FLUCTUATIONS

To demonstrate the robustness of the results against changes in coupling strength, we introduce random fluctuations [20, 35], which can be imposed in the fitness matrix as follows

$$c_{ij} = \begin{cases} X b_{ij} & \text{if } a_{ij} \neq 0 \\ 0 & \text{otherwise } a_{ij} = 0. \end{cases} \quad (4)$$

where X is a uniform random variable lying between 0 and 1. As illustrated in Fig. 2, the bipartite structure evolved through evolution remains unaffected by the random fluctuation in coupling strength. The only implication of having the random fluctuations is that the evolutionary process becomes bit slower. The minima, maxima and mean of R_{\max} decrease during the course of evolution with the mean being bit closer to the minima rather than the maxima (Fig. 2). After few generations, three values become saturated i.e. parallel to the generation axis. The minima does not converge to zero which is unlikely for no fluctuations case. The structural changes during the evolution lead to the decrease in the minima, mean and maxima, whereas $f_{\text{intra}}/f_{\text{inter}}$ still remains close to zero similar to the no fluctuation case.

In order to demonstrate the robustness of results against changes in the initial population networks, we study the evolution of scale-free networks. These networks are generated using Albert-Barabasi model [6] for both the cases of with and without fluctuations in the coupling strength. Since the scale-free networks have randomness arising due to the algorithm, it leads to the appearance of structural variations in different realizations. The given position of blocks in associated adjacency matrices have sufficient variations, as a result the crossed child matrices in GA attain conformation structure leading to bipartite arrangement. For coupling with random fluctuations, there is again an emergence of the bipartite structure (Fig. 5).

We have also analyzed the case when the directed networks form the initial population for the GA. For random directed networks, there would be a very less probability of finding un-directional ($A_{ij} = A_{ji}$) coupling and this probability is dependent on the size and average degree of the network. However, in real world networks, such un-directional couplings are found with very high

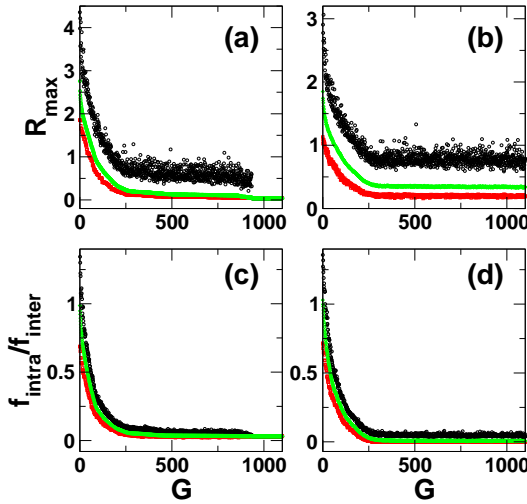


FIG. 5: (Color online) Evolution of bipartite structure for system having both types of the nodes, same as that of Fig. 2 for SF networks. Initial SF networks have $\langle k \rangle = 6$ for $N = 100$. The network population used in GA is 500. (a) and (c) present the evolution of R_{\max} and $f_{\text{intra}}/f_{\text{inter}}$, respectively, for fitness matrix given as Eq. 2, whereas (b) and (d) present the evolution of these quantities for fitness matrix being represented by Eq. 4.

probability [36]. For initial networks being directed, the evolved networks exhibit bipartiteness as exhibited by undirected initial networks as long as the child networks of each generation preserve directionality possessed by the parent networks. The evolution to the bipartiteness as a result of stability maximization directly follows from the discussions around Eq. 3. The only difference is that it requires more number of generations to obtain the evolved networks as compared to the undirected case.

V. ADDITION OF TYPE III NODES AND EMERGENCE OF MULTIPARTITE TROPHIC NETWORKS

The results presented above restrict nodes with only inhibitory and excitatory connections, which is motivated from neural models [26]. If we relax this criterion, nodes may have inhibitory as well as excitatory connections leading to characterization of nodes as type-III (Fig. 6(d)). We investigate the evolution of such type of networks under GA. Starting with a matrix consisting of 1 and -1 entries randomly distributed, which corresponds to all nodes being type-III, there may be some rows having more 1 and some rows having more -1 entries. Now we select a row having more 1 entries and with probability p convert -1 entries into 1 entries. Similarly, for rows having more -1 entries, with probability p we convert 1 entries into -1 entries. The value of p being zero corresponds to the original matrix which we have started with denoting all type-III category nodes, whereas $p = 1$ leads to the situation where those rows

having more 1 entries in the initial matrix, have all their -1 entries converted into 1 corresponding to type-I nodes and those rows having more -1 entries in the initial matrix, have all their 1 entries converted into -1 corresponding to type-II nodes. We find that with increase in p , there is increase in bipartiteness in the evolved networks (Fig. 6(a)).

In the above case, for all values of p either we have only type-III nodes or type-I and type-II nodes with a feeble probability of co-existence of all three types. Whereas in a realistic situation, for instance in ecological systems, there exist few species which are only prey (type-I), few others which are only predator (type-II) and some more species which are prey to some species and act as predators for others (type-III), for example, the herbivores in the grassland food web [30]. In order to mimic this realistic situation which is a mixture of all three types, we consider some of the nodes as type-I, some of the nodes as type-II and rest as type-III. Again type-I nodes will lead to all 1 entries and type-II nodes will lead to all -1 entries in the behavior matrix. In rows corresponding to type-III nodes, 1 and -1 entries are introduced with the equal probability.

We find that with an increase in the generations,

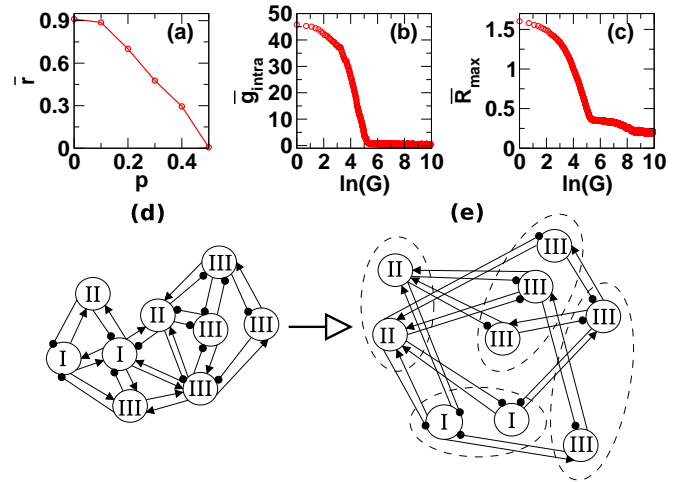


FIG. 6: (Color online) (a) The average value of $f_{\text{intra}}/f_{\text{inter}}$ for the evolved bipartite networks as a function of p . The population at each step consists of 500 networks. (b) The value of g_{intra} , the total number of edges among type-I and type-II nodes, with the evolution. Zero value of g_{intra} indicates formation of different trophic levels consisting type-I and type-II nodes each. (c) Average behavior of R_{\max} over network population with the evolution. Calculations are done for the size of network being 100 with type-I, type-II and type-III being 20, 20 and 60, respectively. Network population used for (b)-(c) is 1000, with size of each network being 100 and average degree 6. For all the cases, $[c_{ij}]$ matrices are defined by Eq. 4. (d) Initial population of ER networks when all three types of nodes (type-I, type-II and type-III) coexist (e) finally evolved structure consisting different trophic levels (denoted with dashed circles). Dots and arrows represent I and E links, respectively.

connections within type-I nodes and connections within type-II nodes decrease and converge towards zero (Fig. 6(b) and Fig. 6(e)). This leads to a situation when type-I nodes have type-II or type-III neighbors and type-II nodes have type-I or type-III neighbors. GA minimizes R_{\max} with relatively faster rate in the beginning of the evolution and as the evolution progresses the rate becomes slower (Fig. 6(c)) due to a steep decrease in the value of τ [25]. Further, number of the type-III nodes, which are neighbors of the type-I nodes but are not neighbors of the type-II or vice versa, are maintained with random fluctuations in the course of evolution. Additionally, with the evolution, the number of connections among such type-III nodes decreases. The nodes of type-I and type-II are not connected within their groups and thus form two distinct trophic levels (Fig. 6(e)). Also, the type-III nodes which are neighbors of type-I (type-II) nodes but are not the neighbors of type-II (type-I) nodes (Fig. 6(e)), form other trophic level(s) [13, 14].

VI. CONCLUSION

To conclude, we present an evolutionary origin of the emergence of bipartiteness in interaction patterns. The essence of the method lies in the property that individuals get classified in to different classes in which they have fixed invariant behaviors. The R_{\max} values are dependent on network architecture as well as fluctuations in coupling strength. Since R_{\max} quantifies the stability of a system [21], there arises a chance of this value to

increase, making a system unstable. Additionally, an increase in the system size may also lead to an increase in R_{\max} implying further that a system with larger size ideally should not exist [21]. However, our results suggest that despite larger system size and high disorder in coupling strength, a balance of I and E limits R_{\max} in the evolved networks, and as a result the fluctuations may not destabilize the system. This result provides an insight in to why despite possessing high degree of disorder ecosystems are robust, which can be attributed to the existence of various trophic levels of species preserving stability of the system.

The method considered here may be useful in optimizing various other measures related with structural as well as spectral behavior [37, 38]. The framework can be extended further to derive an evolutionary understanding of how a system's function gets affected by underlying structural patterns. For instance, assortative-disassortative mixing interaction patterns are seen in real world networks [3], evolution of which can be addressed from the stability point of view.

VII. ACKNOWLEDGEMENTS

SJ thanks DST (SR/FTP/PS-067/2011) and CSIR (25(0205)/12/EMR-II) for funding. SKD acknowledges the University grants commission, India for financial support and members of complex systems lab for useful discussions.

- [1] S. A. Levin, Bull. Amer. Math. Soc. **40**, 3 (2003).
- [2] S. Boccaletti *et. al.*, Physics Reports **424**, 175 (2006).
- [3] M. E. J. Newman, SIAM Rev. **45**, 167 (2003).
- [4] E. A. Variano *et. al.*, Phys. Rev. Lett. **92**, 188701 (2004). *Note: The network size considered here is 25 in the GA model.*
- [5] S. Allesina and M. Pascual, Theor. Ecol. **1**, 55 (2008).
- [6] R. Albert and A.-L. Barabási, Rev. Mod. Phys. **74**, 47 (2002).
- [7] D. J. Watts and S. H. Strogatz, Nature **393**, 440 (1998).
- [8] U. Alon, *An Introduction to Systems Biology: Design Principles of Biological Circuits* (Chapman & Hall/CRC, London, 2006).
- [9] S. Suweis, F. Simini, J. R. Banavar and A. Maritan, Nature **500**, 449 (2013).
- [10] R. P. Rohr, S. Saavedra and J. Bascompte, Science **345** (6195), 416 (2014).
- [11] T. Okuyama and J. N. Holland, Ecol. Lett. **11**, 208 (2008).
- [12] R. Milo *et. al.*, Science **303**, 1538 (2004).
- [13] N. D. Martinez *et. al.*, Ecology **80**, 1044 (1999).
- [14] A. Mougi and M. Kondoh, Science **337**, 349 (2012).
- [15] D. P. Reagan, and R. B. Waide, *The Food Web of a Tropical Rain Forest* (1996).
- [16] J. C. Eccles *et. al.*, J. Physiol (Lond) **126**, 524 (1954).
- [17] A. Lazar *et. al.*, Front Comput. Neurosci. **3**, 23 (2009).
- [18] M. N. Economo and J. A. White, PLoS Comput. Biol. **8**, 1 (2012).
- [19] F. Sergio *et. al.*, Annu. Rev. Ecol. Evol. Syst. **39**, 1 (2008).
- [20] S. Allesina and S. Tang, Nature **483**, 205 (2012).
- [21] R. M. May, Nature **238**, 413 (1972).
- [22] J. I. Perotti *et. al.*, Phys. Rev. Lett. **103**, 108701 (2009).
- [23] J. H. Holland, SIAM Journal on Computing **2**, 88 (1973).
- [24] S. Forrest, Science **261**, 872 (1993).
- [25] S. K. Dwivedi and S. Jalan, Phys. Rev. E **90**, 032803 (2014).
- [26] K. Rajan and L. F. Abbott, Phys. Rev. Lett. **97**, 188104 (2006).
- [27] S. Jalan and S. K. Dwivedi, Phys. Rev. E. **89**, 062718 (2014).
- [28] W. M. Schaffer and M. L. Rosenzweig, Theor. Popul. Biol. **14**, 135 (1978).
- [29] P. Van Mieghem, *Graph Spectra for Complex Networks* (Camb. Uni. Press, 2011).
- [30] E. Estrada and J. A. Rodríguez-Velázquez, Phys. Rev. E **72** 046105 (2005).
- [31] P. Holme *et. al.*, Phys. Rev. E. **68**(5), 056107 (2003).
- [32] S. Jalan *et. al.*, Phys. Rev. E **84**, 046107 (2011).
- [33] H. Sompolinsky *et. al.*, Phys. Rev. Lett. **61**, 259 (1988).

- [34] K. Tun *et. al.*, BMC Bioinf **7**, 24 (2006).
- [35] Z. Yuan *et. al.*, Nature Communications **4**, 2447 (2013).
- [36] M. Hagen *et al.*, Adv. Ecol. Res. **46**, 89 (2012).
- [37] Y.-Y. Liu *et. al.*, Nature **473**, 167 (2011).
- [38] Gang Yan *et. al.*, Phys.Rev. Lett. **108**, 218703 (2012).